Determination of the CKM angle γ in $B^{\pm} \to DK^{\pm}, D\pi^{\pm}$ decays and strong phase determination of $D \to K^+K^-\pi^+\pi^-$ at BESIII

Martin Duy Tat

5th May 2021

Abstract

Write abstract at the end

1 Introduction

In the Standard Model, CP-violation can occur if the CKM matrix has a non-trivial weak phase. This is studied by measuring the lengths and angles of the Unitary Triangle of the CKM matrix. In particular, the angle $\gamma = \arg(-V_{ud}V^*ub/V_{cd}V^*cb)$ is the only angle that can be measured at tree level, with negligible theoretical uncertainties. A precise determination of γ is therefore a good Standard Model benchmark which can be compared with indirect determinations from other CKM observables that are sensitive to new physics.

Sensitivity to γ can be achieved through interference between the $b \to c\bar{u}s$ and $b \to u\bar{c}s$ transitions. A powerful decay mode is $B^{\pm} \to DK^{\pm}$, where D, a superposition of D^0 and $\bar{D}^0$, subsequently decays to a self-conjugate state. This is illustrated in Fig. 1. On the left, the colour favoured decay $B^- \to D^0K^-$ is shown, while on the right is the decay colour suppressed $B^- \to \bar{D}^0K^-$. Interference is observed when D^0 and $\bar{D}^0$ decays to a common final state.

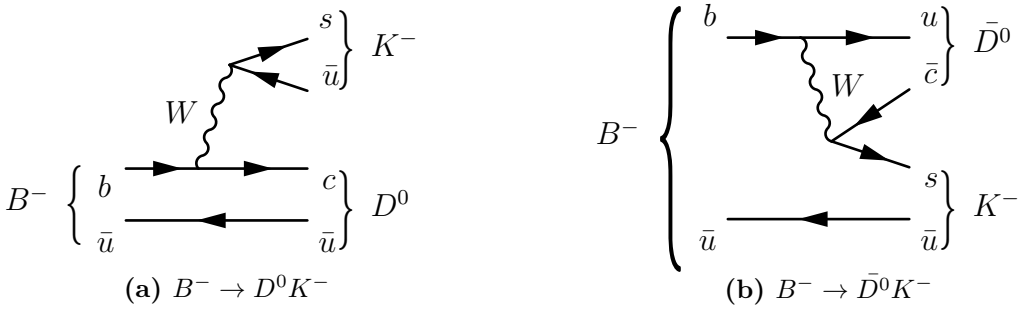

(a) $B^- \to D^0K^-$ **(b)** $B^- \to \bar{D}^0K^-$

Figure 1: Feynman diagrams of $B^- \to DK^-$ decays

A wide range of subsequent D decays has been studied. Most recently, the measurement $\gamma = (68.7^{+5.2}_{-5.1})^\circ$ from an analysis of the decay modes $D \to K^0_S\pi^+\pi^-$ and $D \to K^0_SK^+K^-$ was obtained, which is the single most precise measurement of γ. In this project, the decay $B^{\pm} \to DK^{\pm}$, where $D \to K^+K^-\pi^+\pi^-$, is considered. An initial

study showed that a precision of 14° is achievable with a sample of 1000 $B^{\pm} \to DK^{\pm}$ candidates. From similar decay channels, it is estimated that 2000 candidates can be reconstructed from the combined Run 1+2 LHCb dataset.

A significant challenge with this analysis is that the $D \to K^+K^-\pi^+\pi^-$ decay is a multi-body decay, so the strong phase difference between the D^0 and $\bar{D}^0$ decays varies non-trivially across phase space. Moreover, with four particles in the final state phase space becomes five-dimensional. To predict this strong phase difference, a decay model, such as one developed by LHCb, may be used. However, such a model introduces systematic uncertainties due to modelling.

In this analysis, a model-independent approach is chosen, in which strong phases are determined at a charm factory, BESIII, where, quantum correlated $D^0\bar{D}^0$ pairs are produced at the $\psi(3770)$ resonance. The amplitude-averaged strong phases are measured in bins of the $D \to K^+K^-\pi^+\pi^-$ phase space. The choice of binning scheme may enhace the sensitivity to γ. However, a poor choice of binning scheme may only decrease the statistical sensitivity, but not bias the result. With a model-independent approach, one therefore eliminates the systematic uncertainty due to modelling.

2 Formalism

2.1 γ sensitity through $B^{\pm}$ decays

The amplitude of $B^{\pm} \to DK^{\pm}$ is a coherent sum of the diagrams in Fig. 1,

$$\mathcal{A}(B^- \to DK^-) = \mathcal{A}_D + r_B^{DK} e^{i(\delta_B^{DK} - \gamma)} \mathcal{A}_{\bar{D}}, \tag{2.1}$$

$$\mathcal{A}(B^+ \to DK^+) = \mathcal{A}_{\bar{D}} + r_B^{DK} e^{i(\delta_B^{DK} + \gamma)} \mathcal{A}_D, \tag{2.2}$$

where r_B is the relative magnitude of the diagrams in Fig. 1 and $A_{D,\bar{D}}$ are the amplitudes for the D decay as a function of phase space. δ_B^{DK} is the strong phase of the $B^{\pm} \to DK^{\pm}$ decay and is invariant under CP, while γ is the weak phase that swaps sign under CP.

The $B^{\pm} \to DK^{\pm}$ decay rate is considered in $2 \times N$ bins of phase space, labelled $i = -N, ..., N$, excluding zero. Bin i is related to $-i$ by a CP transformation. When integrating the square of Eqs. (2.1)-(2.2), the $B^- \to DK^-$ decay rate in bin i and $B^+ \to DK^+$ decay rate in bin $-i$ are

$$\Gamma_i^- = h_{B^-}\left[F_i + \left((x_-^{DK})^2 + (y_-^{DK})^2\right)F_{-i} + 2\sqrt{F_i F_{-i}}\left(x_-^{DK} c_i + y_-^{DK} s_i\right)\right], \tag{2.3}$$

$$\Gamma_{-i}^+ = h_{B^+}\left[F_i + \left((x_+^{DK})^2 + (y_+^{DK})^2\right)F_{-i} + 2\sqrt{F_i F_{-i}}\left(x_+^{DK} c_i + y_+^{DK} s_i\right)\right], \tag{2.4}$$

where

$$c_i = \frac{\int_i \mathrm{d}\mathbf{x}\, |\mathcal{A}_D||\mathcal{A}_{\bar{D}}| \cos(\Delta\delta_D)}{\sqrt{\int_i \mathrm{d}\mathbf{x}\, |\mathcal{A}_D|^2 \int_i \mathrm{d}\mathbf{x}\, |\mathcal{A}_{\bar{D}}|^2}}, \quad s_i = \frac{\int_i \mathrm{d}\mathbf{x}\, |\mathcal{A}_D||\mathcal{A}_{\bar{D}}| \sin(\Delta\delta_D)}{\sqrt{\int_i \mathrm{d}\mathbf{x}\, |\mathcal{A}_D|^2 \int_i \mathrm{d}\mathbf{x}\, |\mathcal{A}_{\bar{D}}|^2}}, \quad F_i = \frac{\int_i \mathrm{d}\mathbf{x}\, |\mathcal{A}_D|^2}{\sum_i \int_i \mathrm{d}\mathbf{x}\, |\mathcal{A}_D|^2}. \tag{2.5}$$

c_i and s_i is the strong phase difference $\Delta\delta_D$ between the $B^- \to D^0K^-$ and $B^+ \to \bar{D}^0K^+$ decays, amplitude-averaged over bin i. F_i is the fractional yield of $B^- \to D^0K^-$ in

bin i, and assuming CP conservation in D decays the corresponding fractional yield of $B^+ \to D^0 K^+$ in bin i is F_{-i}. $h_{B^\pm}$ are a normalization constants.

Furthermore, we define the CP observables

$$x_\pm^{DK} = r_B^{DK} \cos\Big(\delta_B^{DK} \pm \gamma\Big), \quad y_\pm^{DK} = r_B^{DK} \sin\Big(\delta_B^{DK} \pm \gamma\Big). \tag{2.6}$$

Therefore, by counting the number of $B^\pm \to DK^\pm$ decays in bins of phase space, one can do a simultaneous fit of Eqs. (2.3)-(2.4) one can obtain the CP observables $x_\pm^{DK}$ and $y_\pm^{DK}$. It is the interference terms in Eqs. (2.3)-(2.4) which causes CP-violation. A clever choice of binning scheme will enhance these interferences, which makes the fit more sensitive to the CP-observables, which can then be interpreted in terms of γ, δ_B^{DK} and r_B^{DK}.

The fit will require external inputs for c_i and s_i from BESIII. In addition, the F_i may either be obtained from flavour tagged D decays, or treated as floating variables in the fit. In this analysis, the second method is preferred in order to reduce systmatic uncertainties due to differences in phase space efficiencies. However, to constrain the F_i and improve the fit stability, the analogous decay mode $B^\pm \to D\pi^\pm$, which has a similar selection and detector signature, is also included as a signal mode in the simultaneous fit. The common topology also means the F_i will be the same, but this mode has a much smaller CP-violation due to interference because $r_B^{D\pi}$ is expected to be much smaller than r_B^{DK}.

2.2 Strong phase and quantum correlations

The strong phase differences $\Delta\delta_D$ of $D \to K^+K^-\pi^+\pi^-$ decays are directly measured in quantum correlated $D^0\bar{D}^0$ decays, using the method of double tagging. This method involves reconstructing either one or both D meson decays. If one of the D mesons is reconstructed in some mode final state f, one can obtain the single tag yield of f. If both D decays are reconstructed in final states f and g, the corresponding double tag yield is obtained. The double tag method is useful when one of the D mesons is reconstructed as $D \to K^+K^-\pi^+\pi^-$, known as the signal mode, and the other D meson decays to a known tag mode.

In particular, if the tag mode is a flavour tag, such as $K^-\pi^+$, one can deduce, through quantum correlations, the original flavour of the D meson on the signal side. One can therefore define a quantity K_i, which is yield of flavour tagged $D^0 \to K^+K^-\pi^+\pi^-$ events in bin i. The corresponding yield for $\bar{D}^0$ decays are then placed in bin $-i$.

The sensitivity to the cosine of the strong phase occurs when the tag mode is a CP eigenstate, or some self-conjugate state with known CP-even fraction F_+. The yield of CP tagged $D \to K^+K^-\pi^+\pi^-$ events in bin i is given by

$$M_i^\pm = \frac{S_\pm}{2S_f}\Big[K_i - 2c_i(2F_+ - 1)\sqrt{K_iK_{-i}} + K_{-i}\Big], \tag{2.7}$$

where $S\pm$ and S_f are the single tag yields of the CP and flavour tag modes used, respectively. For CP even (odd) modes, $F_+ = +1$ (-1). To get sensitivity to the sine of the strong phase, the tag mode must be a self-conjugate mode, and the analogous expression is

$$M_{ij} = \frac{N_{D\bar{D}}}{2S_fS'_f}\Big[K_iK'_{-j} + 2\sqrt{K_iK'_{-j}K_{-i}K'_j}(c'_ic_j + s'_is_j) + K_{-i}K'_j\Big], \tag{2.8}$$

where $N_{D\bar{D}}$ is the total number of $D^0\bar{D}^0$ pairs produced. Here both final states f and f' are reconstructed in bins (i, j) of phase space. In the simplest case, $f = f' = K^+K^-\pi^+\pi^-$, in which $c_i' = c_i$ and $s_i' = s_i$ are all obtained from a fit. One can also choose $f = K^+K^-\pi^+\pi^-$ and $f' = K_S\pi^+\pi^-$, for which the strong phases are already well known.

Once all single and double tag yields have been extracted, a maximum likelihood fit is performed to obtain c_i and s_i. A table of all tag modes is shown in Table 1.

Table 1: Tag modes used in the BESIII double tag analysis. Subsequent decays are shown in parentheses. CP conjugates of flavour modes are implied.

Flavour	CP even	CP odd	Self conjugate
$K^-\pi^+$, $K^-\pi^+\pi^0$, $K^-\pi^+\pi^-\pi^+$, $K^-e^+\nu_e$	K^+K^-, $\pi^+\pi^-$, $\pi^+\pi^-\pi^0$, $K^0_S\pi^0\pi^0$, $K^0_L\pi^0$, $K^0_L\eta(\gamma\gamma)$, $K^0_L\omega(\pi^+\pi^-\pi^0)$	$K^0_S\pi^0$, $K^0_S\phi$, $K^0_S\eta(\gamma\gamma, \pi^+\pi^-\pi^0)$, $K^0_S\omega(\pi^+\pi^-\pi^0)$, $K^0_S\eta'(\pi^+\pi^-\eta(\gamma\gamma), \pi^+\pi^-\gamma)$	$K^0_S\pi^+\pi^-$, $K^+K^-\pi^+\pi^-$

Currently, BESII has collected 2.932 fb of data at the $\psi(3770)$ resonance during 2010-2011, which is unsufficient for doing a maximum likelihood fit. However, a significant increase in data is expected from 2022, allowing for a precise determination of c_i and s_i.

3 LHCb detector

The LHCb is a single arm forward spectrometer designed to study beauty and charm hadrons in pp collisions at the LHC. The main components important for this analysis are the high precision tracking system and the two Ring Imaging Cherencov counters (RICH1 and RICH2).

The tracking system includes the Vertex Locator (VELO). The VELO consists of silicon strip modules close to the interaction point, which provides high precision tracking and identification of displaced secondary vertices that are important for beauty and charm physics. A dipole magnet with bending power of about 4 T m together with three tracking stations of silicon strip detectors and straw drift tubes placed downstream provides a measurement of the momentum of charged particles with an uncertainty of 0.5% at low momentum at 1.0% at 200 GeV. The impact parameter is measured with a resolution of $(15 + 29/p_T)\mu$m, where p_T is the transverse momentum.

The two RICH detectors, together with the tracking system and the calorimeter system, separates kaons from pions. The upstream RICH1 detector covers the lower momentum range up to 60 GeV while the downstream RICH2 covers the higher momentum range from 15 GeV to 100 GeV.

To model the kinematic distributions of signal and background components and determine selection efficiencies, simulations of pp collisions are generated in Pythia. Decays are described by EvtGen and final state radiation is generated witih Photos. In addition, models of decay amplitudes are incorporated using the AmpGen framework.

4 Binning scheme

In a three-body decay, such as $D \to K^0_S\pi^+\pi^-$, the two-dimensional phase space may be visualized in a two-dimensional Dalitz plot. In an analysis analogous to $D \to K^+K^-\pi^+\pi^-$,

the Dalitz space was separated into bins of similar strong phase, such that the amplitude-averaged strong phases c_i and s_i were not diluted due to binning. In addition, the Dalitz plot was split symmetrically into bins with positively and negatively indexed bins, such that mainly Cabbibo favoured resonances and doubly suppressed Cabbibo resonances were on opposite sides of each other. Such a clever choice of bins will therefore enhance the interference terms in Eqs. (2.3)-(2.4), and thus enhance the sensitivity to CP-violation effects.

A similar choice of binning must be determined for the four-body decay mode $D \to K^+K^-\pi^+\pi^-$. While similar in many ways, this phase space is five-dimensional and cannot easily be visualized. Instead, an amplitude model is used to predict the decay amplitude and strong phase difference. The model, implemented using the AmpGen framework, takes in the momenta of the D daughter particles, and the output is used to calculate the $D \to K^+K^-\pi^+\pi^-$ decay amplitude $\mathcal{A}(D)$. One can then define

$$\frac{\mathcal{A}(D^0)}{\mathcal{A}(\bar{D}^0)} \equiv r_D e^{i\Delta\delta_D}, \tag{4.1}$$

where $\Delta\delta_D$ is the strong phase difference and r_D is the relative magnitude, both of which vary across phase space. A convenient binning scheme would therefore be equal $\Delta\delta_D$ separation in each bin such that areas of phase space with similar strong phases are grouped together in the same bins.

Under a CP transformation, $\Delta\delta_D \to -\Delta\delta_D$ and $\ln(r_D) \to -\ln(r_D)$. For $\ln(r_D) > 0$, the $\bar{D}^0 \to K^+K^-\pi^+\pi^-$ decay is suppressed, relative to $D^0 \to K^+K^-\pi^+\pi^-$, while the converse is true for $\ln(r_D) < 0$. The interference terms in Eqs. (2.3)-(2.4) may therefore be enhanced if the positively and negatively indexed bins are split along the line $\ln(r_D) = 0$.

A measure of the binning scheme sensitivity to CP observables is taking the ratio of the statistical sensitivity to $x_\pm$ and $y_\pm$ in a binned fit and the corresponding statistical sensitivity with infinitely many bins. It can be shown that

$$Q^2 = \frac{1}{2}\Big(Q_+^2 + Q_-^2\Big), \quad Q_\pm^2 = 1 - \sum_i \frac{F_i F_{-i}\Big(1 - c_i^2 - s_i^2\Big)}{N_i^\pm}, \tag{4.2}$$

where $N_i^\pm$ are calculated using Eqs. (2.3)-(2.4). To maximize Q, the bin boundaries along $\Delta\delta_D$ are moved symmetrically around $\Delta\delta_D = 0$.

To assess the binning scheme performance, 1000 toy experiments with 2000 $B^\pm$ candidates was generated with the amplitude model using AmpGen. The input parameters used were $\gamma = 75$ degree, $\Delta_B = 130°$ and $r_B = 0.1$. An unbinned maximum likelihood fit was performed in order to establish a benchmark for the γ precision obtainable. It was found that the average precision to γ was $\Delta\gamma = 11°$.

For the particular choice of 2×8 bins, the optimal binning scheme is shown in Fig. 2a. Eq. (4.2) gives $Q = 0.90$, which indicates that 10% sensitivity is lost due to binning. A binned maximum likelihood fit was performed using the binning scheme in Fig. 2a and Eqs. (2.3)-(2.4) to extract $x_\pm^{DK}$ and $y_\pm^{DK}$. The parameters c_i, s_i and F_i were calculated using Monte Carlo integration of Eqs. (2.5) with $\mathcal{A}(D)$ calculated using the amplitude model. Finally, γ, δ_B and r_B where obtained by fitting $x_\pm^{DK}$ and $y_\pm^{DK}$ using Eqs. (2.6).

The pull distributions of $x_\pm^{DK}$, $y_\pm^{DK}$ were found to all have a Gaussian shape with zero mean and unit standard deviation.

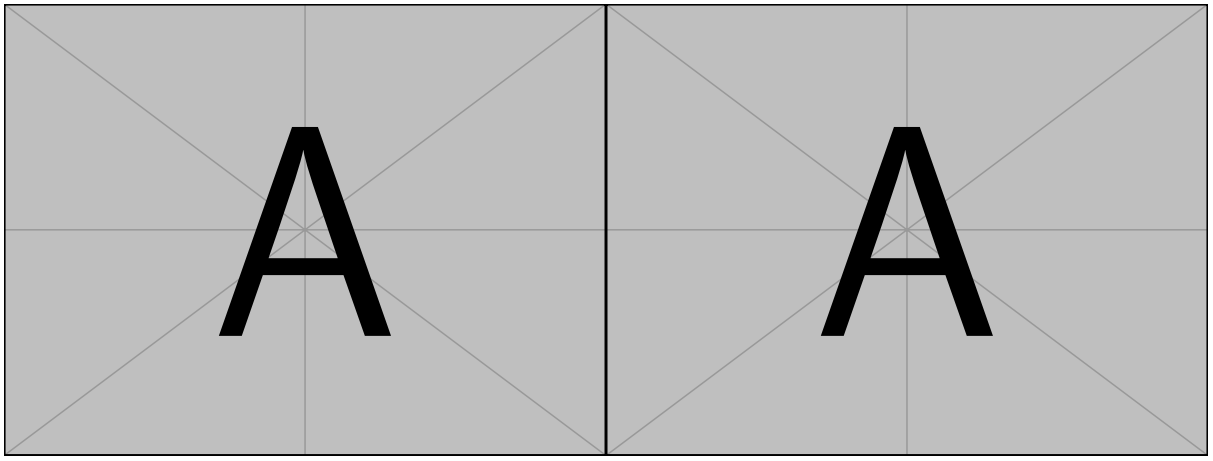

(a) Binning scheme definition for 2×8 bins **(b)** Distribution of γ from toy study

Figure 2

Table 2: The pull distribution mean and standard deviation from toy study.

Observable	Mean	Standard deviation
x_+^{DK}	$(3.7 \pm 3.3) \times 10^{-2}$	$(9.80 \pm 0.26) \times 10^{-1}$
x_-^{DK}	$(1.4 \pm 3.3) \times 10^{-2}$	$(9.48 \pm 0.26) \times 10^{-1}$
y_+^{DK}	$(2.6 \pm 3.4) \times 10^{-2}$	$(10.04 \pm 0.28) \times 10^{-1}$
y_-^{DK}	$(-1.7 \pm 3.1) \times 10^{-2}$	$(9.24 \pm 0.26) \times 10^{-1}$
γ	$(4.9 \pm 3.3) \times 10^{-2}$	$(9.77 \pm 0.29) \times 10^{-1}$
δ_B	$(4.9 \pm 3.3) \times 10^{-2}$	$(9.86 \pm 0.26) \times 10^{-1}$
r_B	$(1.72 \pm 0.32) \times 10^{-1}$	$(9.46 \pm 0.26) \times 10^{-1}$

5 $B^{\pm}$ candidate selection

5.1 Signal candidate requirements

Explain how signal events are selected

5.2 Boosted Decision Tree

Show the performance of the BDT

5.3 Background from $D^0 \to K^-\pi^+\pi^-\pi^+$

Show studies of $K3\pi$ contamination

5.4 Charmless backgrounds

Show how flight significance cut removes $B \to KKK\pi\pi$ and mention that $B \to KK\pi\pi\pi$ is insignificant

6 Fit to extract CP observables

6.1 Global fit and invariant mass spectra

State the fit procedure for global fit and show results of global fit for Run 2, including yields

6.2 Binned CP fit and CP observables

Explain the binned CP fit to extract CP observables

6.3 Validation of fit procedure with toy studies

7 External strong phase input from BESIII

Describe how to extract strong phases at a charm factory and show some initial plots of single tag yields and double tag yields

8 Discussion of future work

Discuss the plan further

9 DPhil thesis plan

Discuss DPhil thesis plan with Guy first!